

RESEARCH ARTICLE

10.1002/2014JD021590

Key Points:

- GEOSCCM has improved its simulation of total column ozone
- By 2100 the SPARC 2013 ODS scenario results in 60 pptv more of Cl_{tot}
- Differences in quasi-global ozone between ODS scenarios is less than 1 DU

Correspondence to:

L. D. Oman,
luke.d.oman@nasa.gov

Citation:

Oman, L. D., and A. R. Douglass (2014), Improvements in total column ozone in GEOSCCM and comparisons with a new ozone-depleting substances scenario, *J. Geophys. Res. Atmos.*, 119, 5613–5624, doi:10.1002/2014JD021590.

Received 30 JAN 2014

Accepted 10 APR 2014

Accepted article online 17 APR 2014

Published online 6 MAY 2014

Improvements in total column ozone in GEOSCCM and comparisons with a new ozone-depleting substances scenario

Luke D. Oman¹ and Anne R. Douglass¹¹Atmospheric Chemistry and Dynamics Laboratory, NASA Goddard Space Flight Center, Greenbelt, Maryland, USA

Abstract The evolution of ozone is examined in the latest version of the Goddard Earth Observing System Chemistry–Climate Model (GEOSCCM) using old and new ozone-depleting substances (ODS) scenarios. This version of GEOSCCM includes a representation of the quasi-biennial oscillation, a more realistic implementation of ozone chemistry at high solar zenith angles, an improved air/sea roughness parameterization, and an extra 5 parts per trillion of CH_3Br to account for brominated very short-lived substances. Together these additions improve the representation of ozone compared to observations. This improved version of GEOSCCM was used to simulate the ozone evolution for the A1 2010 and the new Stratosphere-troposphere Processes and their Role in Climate (SPARC) 2013 ODS scenario derived using the SPARC Lifetimes Report 2013. This new ODS scenario results in a maximum Cl_{tot} increase of 65 parts per trillion by volume (pptv), decreasing slightly to 60 pptv by 2100. Approximately 72% of the increase is due to the longer lifetime of CFC-11. The quasi-global (60°S–60°N) total column ozone difference is relatively small and less than 1 Dobson unit on average and consistent with the 3–4% larger 2050–2080 average Cl_y in the new SPARC 2013 scenario. Over high latitudes, this small change in Cl_y compared to the relatively large natural variability makes it not possible to discern a significant impact on ozone in the second half of the 21st century in a single set of simulations.

1. Introduction

Ozone is a critically important trace gas in the Earth climate system. It is closely connected to the dynamics of the atmosphere as well as the climate [Gillett and Thompson, 2003; McFarlane, 2008]. Since 1994 the World Meteorological Organization (WMO) has conducted a careful review of observations of ozone and related constituents and state-of-the-art simulations every 4 years, most recently producing *Scientific Assessment of Ozone Depletion: 2010* [World Meteorological Organization (WMO), 2011]. While many factors influence the evolution of ozone, changes in the levels of ozone-depleting substances (ODS) and the Brewer-Dobson circulation are important drivers of ozone change [Oman et al., 2010].

Recently, a new assessment of the lifetimes of many ODS was undertaken by the World Climate Research Program's project Stratosphere-troposphere Processes and their Role in Climate (SPARC) [SPARC, 2013], leading to a new ODS scenario based on the latest scientific understanding. One of the larger changes was to the lifetime of $CFCl_3$ (CFC-11, F11 hereafter), which was reassessed to be 52 years from 45 years based on Kaye et al. [1994]. This longer lifetime results in higher atmospheric loading of F11 in the 21st century. Velders and Daniel [2014] produced a new mixing ratio-based boundary condition ODS scenario based on the reassessed F11 lifetime and a number of other species. They found a higher level of equivalent effective stratospheric chlorine (EESC), which is the total effective amount of chlorine and bromine in the stratosphere [Daniel et al., 1995; Newman et al., 2007], mainly during the second half of the 21st century as compared to the previous A1 2010 scenario [WMO, 2011].

In addition to halogen loading, possible Brewer-Dobson circulation changes in response to climate change [Butchart et al., 2011] could have important impacts on ozone and other atmospheric constituents [Oman et al., 2010]. The evidence for changes in the Brewer-Dobson circulation has so far been mixed, with some studies showing little if any change [Engel et al., 2009; Ray et al., 2010] to others suggesting significant tropical lower stratospheric changes [Randel and Thompson, 2011; Kawatani and Hamilton, 2013] over the most recent decades.

The quasi-biennial oscillation (QBO) is a leading mode of variability in the tropical stratosphere [Baldwin et al., 2001]. The QBO modulates deep tropical upwelling and temperature, which strongly impacts the variability

Table 1. Simulations Used in This Study

Name	Years	SST/SIC	GHG	ODS	+5 Br _y	QBO	Figures
GEOS-4_o	1960–2004	Obs. ^a	Obs. ^a	Obs. ^a	No	No	1 and 2
GEOS-5_old_o	1960–2005	Obs. ^a	Obs. ^a	Obs. ^a	No	No	1 and 2
GEOS-5_new_o	1960–2012	Obs. ^a	Obs. ^a	Obs. ^a	Yes	Yes	1 and 2
GEOS-4_m	1972–2098	CCSM3 ^b	A1B ^d	A1 2002 ^f	No	No	3 and 4
GEOS-5_old_m	1960–2099	CCSM3 ^b	A1B ^d	A1 2006 ^g	No	No	3 and 4
GEOS-5_new_m	1960–2099	CESM1 ^c	RCP6.0 ^e	SPARC 2013 ^h	Yes	Yes	3 and 4
P_A1_2010	1960–2012	Obs. ^a	Obs. ^a	Obs. ^a	Yes	Yes	6, 7, and 8
PF_A1_2010	1960–2099	CESM1 ^c	RCP6.0 ^e	A1 2010 ⁱ	Yes	Yes	5b, 6, 7, 8, 9, and 10
PF_SPARC_2013	1960–2099	CESM1 ^c	RCP6.0 ^e	SPARC 2013 ^h	Yes	Yes	5b, 6, 7, 8, 9, and 10

^aObs. refers to Observations.

^bCommunity Climate System Model version 3 (CCSM3).

^cCommunity Earth System Model version 1 (CESM1).

^dA1B refers to the Intergovernmental Panel on Climate Change (IPCC)/Special Report Emission Scenario A1B.

^eRCP6.0 refers to the Intergovernmental Panel on Climate Change/Representative Concentration Pathways Scenario 6.0 (IPCC/RCP6.0).

^fA1 2002 refers to the WMO 2002 Ozone Assessment ODS scenario A1.

^gA1 2006 refers to the WMO 2006 Ozone Assessment ODS scenario A1.

^hSPARC 2013 refers to the new ODS scenario derived using the SPARC lifetimes Report 2013.

ⁱA1 2010 refers to the WMO 2010 Ozone Assessment ODS scenario A1.

of ozone and many other constituents and influences the mean state of ozone as well as other constituents [Hurwitz *et al.*, 2013]. Simulation of a realistic QBO is a new feature for the Goddard Earth Observing System version 5 (GEOS-5) general circulation model and when coupled with a chemistry module allows the examination of the QBO impact on trace gas constituents [Hurwitz *et al.*, 2013]. This and other improved capabilities in the latest version of GEOS Chemistry-Climate Model (GEOSCCM) are examined here, focusing mainly on total column ozone.

The main goals of this study are (1) to document the improvements in ozone in GEOSCCM, (2) to demonstrate the changes due to improvements in GEOSCCM, and (3) to compare the evolution of ozone in the new ODS scenario to that obtained with the previous ODS scenario. Section 2 describes the improved version of GEOSCCM, the boundary condition scenario, and observations of ozone that are compared with simulations. Section 3 discusses the improvements to ozone in GEOSCCM and compares the evolution of ozone in the old and new ODS scenarios. Section 4 summarizes the main results and gives concluding remarks.

2. Model Description, Scenarios, and Measurements

We discuss improvements to the simulation of ozone and examine the evolution of ozone to new and old ODS scenarios in the GEOSCCM. This latest version of GEOSCCM couples the GEOS-5 [Rienecker *et al.*, 2008; Molod *et al.*, 2012] general circulation model to a comprehensive stratospheric chemistry module. Version 4 of GEOS (GEOS-4) with stratospheric chemistry was discussed in detail in Pawson *et al.* [2008], and any changes that significantly impact ozone and related species since that paper are detailed below. The GEOS-5 simulations described in this study all use a horizontal resolution of 2° latitude and 2.5° longitude with 72 vertical layers up to 0.01 hPa (80 km); the GEOS-4 simulation has the same horizontal resolution and vertical domain but only 55 layers. Table 1 gives an overview of the simulations considered in this study, including simulation length, forcings applied, whether or not there was a QBO, and the figures associated with each simulation.

GEOSCCM has been extensively evaluated using process-oriented diagnostics in both Chemistry-Climate Model Validation 1 (CCMVal-1) [Eyring *et al.*, 2006] and CCMVal-2 [SPARC Chemistry-Climate Model Validation (CCMVal), 2010]. GEOSCCM has performed well in both chemical- and transport-related processes [SPARC CCMVal, 2010; Strahan *et al.*, 2011; Douglass *et al.*, 2012], but noted deficiencies include the following: the lack of a QBO, late breakup of the Antarctic vortex, and high bias in high-latitude ozone. The latest version of GEOSCCM includes significant improvements to most of these deficiencies.

GEOSCCM now internally generates the QBO [Hurwitz *et al.*, 2013] with realistic periodicity and magnitude as a result of improvements to the nonorographic gravity wave drag scheme. Revisions to the air/sea roughness parameterization [Garfinkel *et al.*, 2011, 2013] improved the surface wind speeds, especially over the Southern

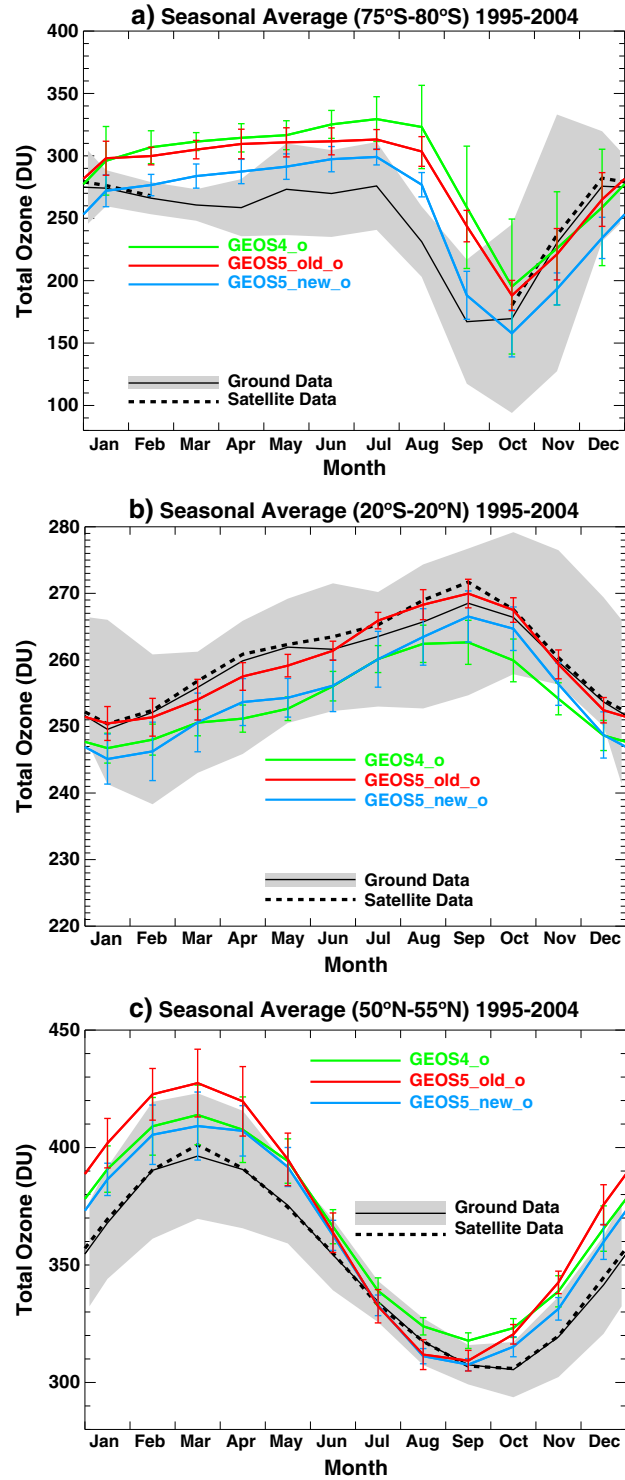


Figure 1. The annual cycle of total column ozone averaged between 1995 and 2004 over (a) 75–80°S, (b) 20°S–20°N, and (c) 50–55°N for GEOS-4_o (green curve), GEOS-5_old_o (red curve), GEOS-5_new_o (light blue curve), and both ground-based (solid black curve) and satellite-derived (dashed black curves) measurements. The gray-shaded areas around the ground-based data and color whiskers on the simulations are ± 2 standard deviations.

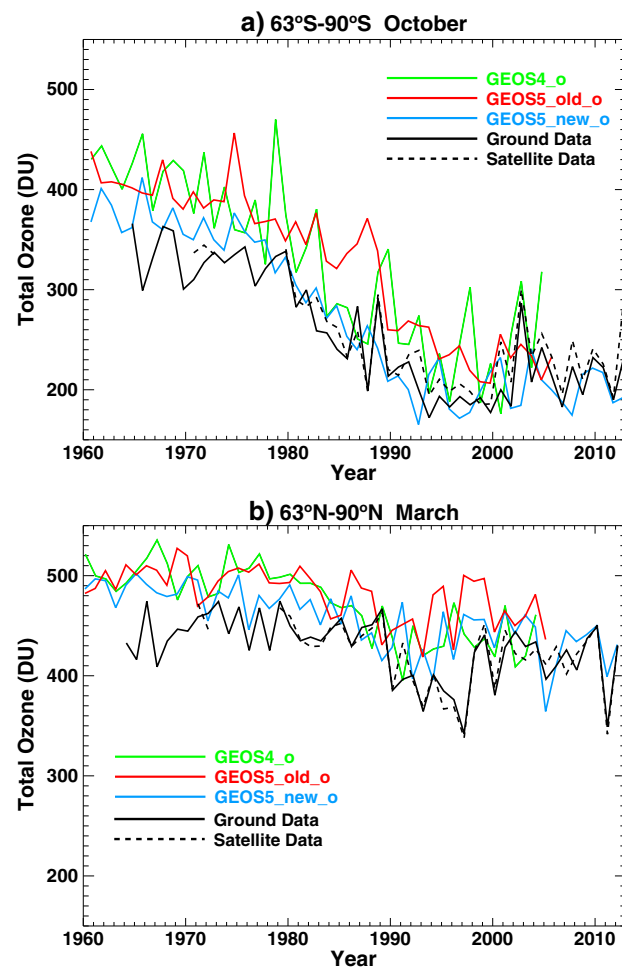


Figure 2. Total column ozone (DU) over area-weighted polar cap averages for (a) 63–90°S during October and (b) 63–90°N during March for GEOS-4_o (green curve), GEOS-5_old_o (red curve), GEOS-5_new_o (light blue curve), and both ground-based (solid black curve) and satellite-derived (dashed black curves) measurements.

Ozone observations used in this study come from satellites and ground-based observing networks. The satellite observations are from the Total and Profile Merged Ozone Data Set version 8.6 [Bhartia *et al.*, 2013; Stolarski and Frith, 2006; Ziemke *et al.*, 2005] (http://acbd-ext.gsfc.nasa.gov/Data_services/merged/index.html), and the ground-based total column ozone (TCO) measurements are updated from Fioletov *et al.* [2002, 2008].

3. Results and Discussion

3.1. Ozone and Tropical Upwelling in GEOSCCM

We first focus on how the ozone and tropical upwelling have evolved between previous versions of GEOSCCM and the current version. For Figures 1–4, the green curve (labeled GEOS-4_o or GEOS-4_m) is from the version used in CCMVal-1, red curve (GEOS-5_old_o or GEOS-5_old_m) is from CCMVal-2, and the light blue curve (GEOS-5_new_o or GEOS-5_new_m) is the latest version that includes the QBO and additional changes discussed in section 2. GEOS-5_new is the same version that is used to produce the two ODS scenarios simulations discussed later.

First, we examine the seasonal cycle in the Northern Hemisphere (NH) midlatitudes, tropics, and Southern Hemisphere (SH) high latitudes compared to both ground- and satellite-based estimates of TCO. We use

Ocean, and reduced the late breakup of the Antarctic polar vortex. Significant improvements in the simulation of ozone have also resulted from allowing the transition from day/night chemistry to occur at a maximum solar zenith angle of 94° rather than the 90° used previously. An extra 5 parts per trillion (ppt) of CH₃Br is now included to represent very short-lived brominated substances and is in better agreement with observations [Liang *et al.*, 2010]. Observed/modeled stratospheric sulfate surface area densities [Eyring *et al.*, 2013] are used in the new simulations from 1960 to 2011 with 2011 values used for years after 2011. Previous simulations assumed an unperturbed stratospheric aerosol background state from 1979.

The old (A1 2010) and new (SPARC_2013) ODS scenarios are described in Velders and Daniel [2014] and are both constrained by observations in the past (up to ~2008). All of the new GEOSCCM simulations include greenhouse gas (GHG) concentrations from the Representative Concentration Pathway (RCP) 6.0 indicating 6.0 W/m² radiative forcing by 2100 [Meinshausen *et al.*, 2011; Moss *et al.*, 2010]. While the RCPs also provide scenarios of ODS, we are not using them in this study. Sea surface temperature (SST) and sea ice concentrations (SIC) were prescribed from an AR5 simulation using the Community Earth System Model version 1 (CESM1) from 1960 to 2099 [Gent *et al.*, 2011] forced with the same RCP6.0 GHG scenario.

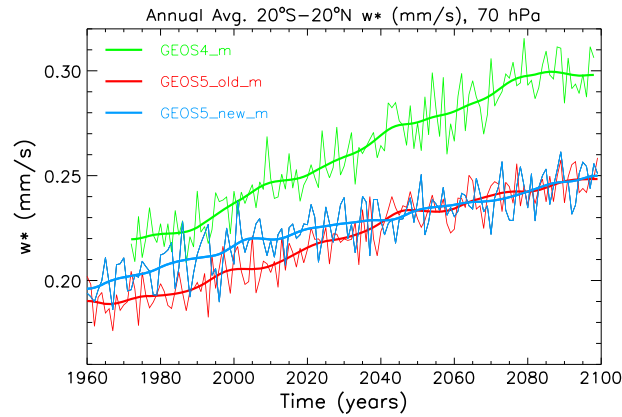


Figure 3. Annual average tropical (20°S–20°N) residual vertical velocity (mm/s) at 70 hPa for GEOS-4_m (green curve), GEOS-5_old_m (red curve), and GEOS-5_new_m (light blue curve). GEOS-4 simulation is from 1972 to 2098, and the GEOS-5 simulations are from 1960 to 2099. The thick lines are output smoothed to remove interannual variability.

round. *Lamago et al.* [2003] noted a similar reduction in ozone when the high solar zenith angles were allowed to impact chemistry in the European Centre/Hamburg 4 model. Figure 1b shows that the tropical (20°S–20°N) ozone is well represented in all versions of GEOSCCM with a small decrease in ozone between GEOS-5_old_o and GEOS-5_new_o. The NH midlatitudes (50–55°N) are shown in Figure 1c with a general high bias outside of boreal summer. This high bias is partially reduced in GEOS-5_new_o compared to GEOS-5_old_o but similar to the GEOS-4_o version.

Next, we compare the past changes in polar total column ozone for October and March for the SH and NH, respectively. Figure 2a shows the area-weighted polar cap (63–90°S) average TCO for October in observations (black solid and dashed curves) and the three versions of GEOSCCM. The main difference in simulations can be seen before 1980 with some reduction in the high bias in the GEOS-5_new_o run. A similar but smaller reduction in high bias is also apparent in the NH polar region (63–90°N) in March; however, some biases still remain. In the SH polar region the root-mean-square (RMS) difference between 1964 and 2004 is 67 Dobson units (DU) for GEOS-4_o and GEOS-5_old_o and is reduced to 39 DU for GEOS-5_new_o compared to ground-

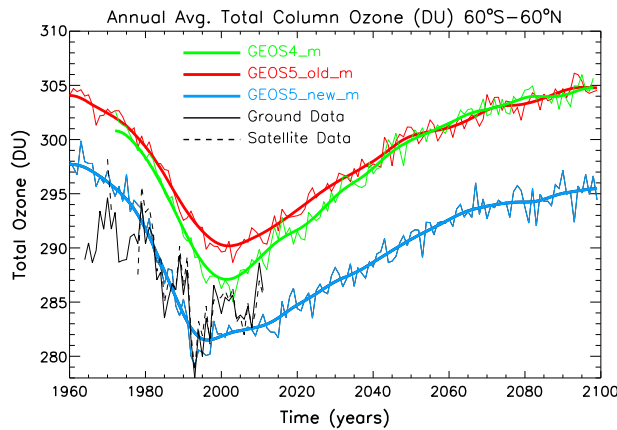


Figure 4. Annual average quasi-global (60°S–60°N) total column ozone (DU) for GEOS-4_m (green curve), GEOS-5_old_m (red curve), GEOS-5_new_m (light blue curve), ground-based measurements (black solid curve), and satellite-based measurements (black dashed curve). GEOS-4_m simulation is from 1972 to 2098, the GEOS-5 simulations are from 1960 to 2099, and the ground-based observations are from 1964 to 2011. The thick lines are output smoothed to remove interannual variability.

the 1995–2004 time period for comparison since it is the common period among all simulations and includes a well-developed ozone hole. Figure 1a shows that the TCO over 75–80°S was very similar for GEOS-4_o and GEOS-5_old_o with both biased high compared to observations for all months other than October–December. The bias was particularly large during the ozone hole onset in August and September. A significant portion of this high bias has been reduced in the GEOS-5_new_o version from two particular changes, allowing the ozone chemistry to continue at high solar zenith angles and the inclusion of an extra 5 ppt of Br_y. The extra Br_y had its largest impact during August and September, whereas the high solar zenith angle change reduced ozone year

round. *Lamago et al.* [2003] noted a similar reduction in ozone when the high solar zenith angles were allowed to impact chemistry in the European Centre/Hamburg 4 model. Figure 1b shows that the tropical (20°S–20°N) ozone is well represented in all versions of GEOSCCM with a small decrease in ozone between GEOS-5_old_o and GEOS-5_new_o. The NH midlatitudes (50–55°N) are shown in Figure 1c with a general high bias outside of boreal summer. This high bias is partially reduced in GEOS-5_new_o compared to GEOS-5_old_o but similar to the GEOS-4_o version.

Next, we compare the past changes in polar total column ozone for October and March for the SH and NH, respectively. Figure 2a shows the area-weighted polar cap (63–90°S) average TCO for October in observations (black solid and dashed curves) and the three versions of GEOSCCM. The main difference in simulations can be seen before 1980 with some reduction in the high bias in the GEOS-5_new_o run. A similar but smaller reduction in high bias is also apparent in the NH polar region (63–90°N) in March; however, some biases still remain. In the SH polar region the root-mean-square (RMS) difference between 1964 and 2004 is 67 Dobson units (DU) for GEOS-4_o and GEOS-5_old_o and is reduced to 39 DU for GEOS-5_new_o compared to ground-

based TCO measurements. In the NH polar region the RMS difference is 53 DU for GEOS-4_o and 62 DU for GEOS-5_old_o and is reduced to 44 DU for GEOS-5_new_o. None of these simulations reproduces the string of low-ozone years seen in observations in the mid-1990s.

The residual vertical velocity (w^*) from 20°S to 20°N at 70 hPa can be used as a proxy for Brewer-Dobson circulation changes. Tropical upwelling changes affect the distributions of ozone [*Li et al.*, 2009; *Oman et al.*, 2010] and other trace gases so that any change in the predicted rate of tropical upwelling increase can impact their distributions. This next set of simulations is with the same three versions of GEOSCCM considered in the previous figures but with modeled SST and SIC. In this study GEOSCCM is not coupled to an interactive ocean, so SST and SIC are

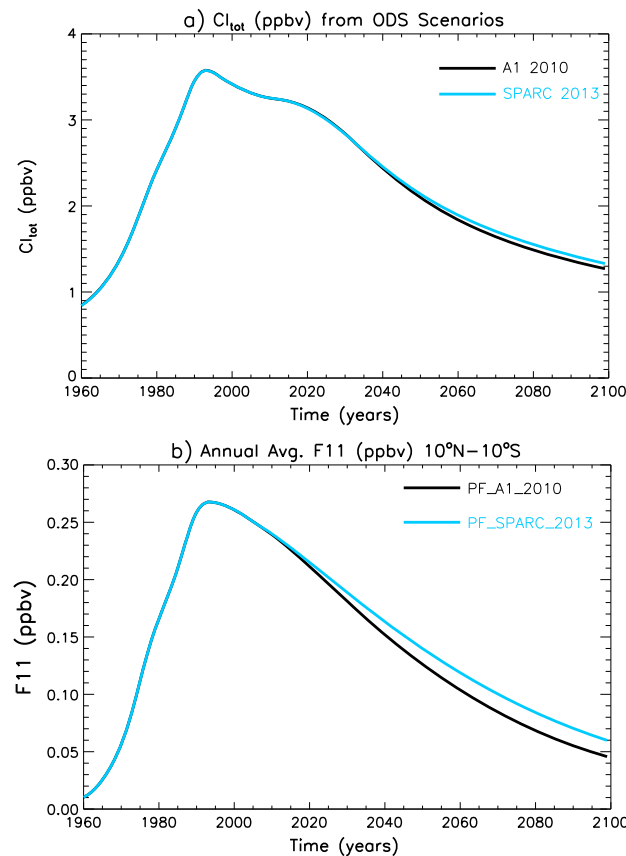


Figure 5. (a) Annual average total chlorine (Cl_{tot}) in ppbv from the A1 2010 (black curve) and SPARC_2013 (light blue curve) ODS scenarios. (b) Annual average F11 concentration (ppbv) in the tropical troposphere from the PF_A1_2010 (black curve) and PF_SPARC_2013 (light blue curve) simulations from 1960 to 2099.

biased compared to ground- and satellite-based observation of the recent past. The high bias is greatly reduced in GEOS-5_new_m. GEOS-5_new_m includes observed/modeled sulfate surface area densities and reproduces the observed decrease in ozone following the Mt. Pinatubo eruption. The average loss is now greatest in the mid-1990s instead of around 2000 in simulations without sulfate surface area density variability and the extra 5 ppt of Br_y . The new simulation also compares better to observations during this same period.

3.2. New ODS Scenario

The total chlorine prescribed by the mixing ratio boundary conditions is shown in Figure 5a for the A1 2010 (black curve) and SPARC 2013 (light blue curve) scenarios. The difference in the two scenarios becomes apparent after 2040 when the SPARC 2013 total chlorine becomes slightly higher. The SPARC 2013 scenario has a maximum difference of 65 parts per trillion by volume (pptv), with 60 pptv more total chlorine than the A1 2010 scenario by 2100. Much of this difference is due to the longer lifetime of F11. Figure 5b shows the annual average concentration of F11 in the two simulations in the tropical troposphere. The difference in the two scenarios is apparent in F11 after about 2015, two decades earlier than it is possible to discern a difference in total chlorine. The longer lifetime in the new scenario leads to 14 pptv more F11 by 2100; since there are three chlorine atoms per F11 molecule, this causes 43 pptv more total chlorine. This represents 72% of the difference in total chlorine by 2100.

3.3. Total Column Ozone Response

Next, we focus on the TCO resulting from three simulations with the latest version (GEOS-5_new) of GEOSCCM. The first simulation (P_A1_2010, orange curves) is for the past and includes observed SST and SIC.

prescribed from Community Climate System Model version 3 (CCSM3) and CESM1 coupled atmosphere ocean simulations (see Table 1). The GEOS-5 simulations span 1960–2099, while the GEOS-4_m simulation was integrated from 1972 to 2098. While all simulations show an increase in tropical upwelling over time (Figure 3), the GEOS-4_m simulation shows the largest increase. This increase is reduced in subsequent versions of the GEOSCCM. It is important to note that while the GEOS-4_m and GEOS-5_old_m simulations use the same SST and A1B GHG scenario, GEOS-5_new_m uses SSTs and GHGs consistent with the RCP6.0 scenario. The differences in tropical SSTs between GEOS-5_old_m and GEOS-5_new_m (not shown) are consistent with the differences in tropical upwelling in these two simulations. There is also little apparent difference in the upwelling interannual variability at 70 hPa between GEOS-5_old_m (no QBO) and GEOS-5_new_m (QBO) over to 20°S–20°N region. This point will be examined in more detail later comparing ozone changes in the deep tropics to the broader tropics.

The annual average quasi-global (60°S–60°N) TCO for the same simulations is shown in Figure 4. GEOS-4_m and GEOS-5_old_m produce values that are high

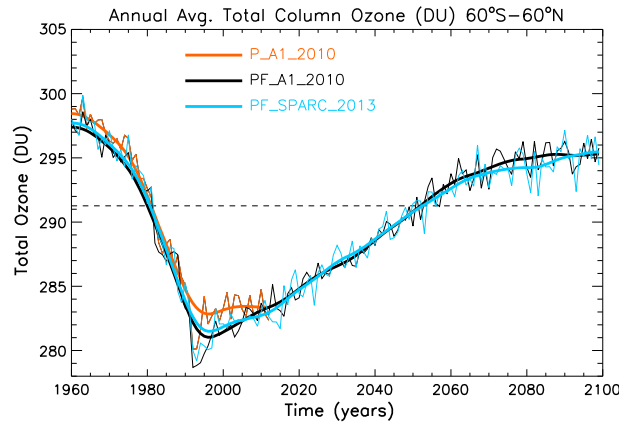


Figure 6. Annual average quasi-global (60°S–60°N) total column ozone (DU) for P_A1_2010 (orange curve), PF_A1_2010 (black curve), and PF_SPARC_2013 (light blue curve) simulations. P_A1_2010 simulation is from 1960 to 2012, and the PF_A1_2010 and PF_SPARC_2013 simulations are from 1960 to 2099. The thick lines are output smoothed to remove interannual variability. The black dashed line indicates the 1980 value of the smoothed PF_A1_2010 simulation.

The second simulation (PF_A1_2010, black curves) includes both past and future but uses modeled SST and SIC from an AR5 simulation with CESM1. The third simulation (PF_SPARC_2013, light blue curve) uses the same SST and SIC as PF_A1_2010 but includes the new ODS scenario.

Evolution of quasi-global TCO is similar for these three simulations (Figure 6) with a few small differences. The simulation with observed SST and SIC (P_A1_2010) has slightly higher TCO, with the largest differences from the other simulations between 1990 and 2010. Evolutions of TCO are similar for the two scenarios with modeled SST and SIC, with somewhat less TCO in the second half of the 21st century in the PF_SPARC_2013

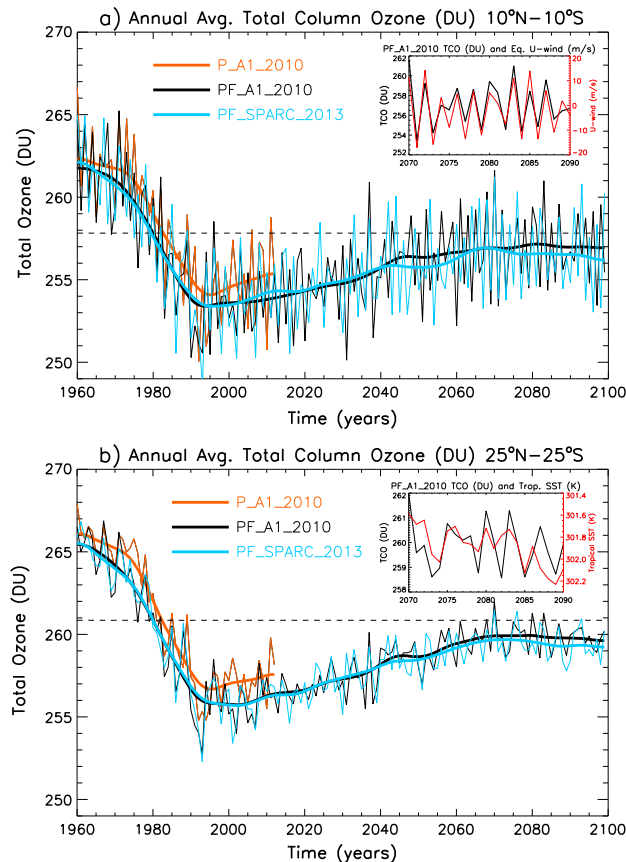


Figure 7. (a) Annual average 10°S–10°N total column ozone (DU) for P_A1_2010 (orange curve), PF_A1_2010 (black curve), and PF_SPARC_2013 (light blue curve) simulations. P_A1_2010 simulation is from 1960 to 2012; the PF_A1_2010 and PF_SPARC_2013 simulations are from 1960 to 2099. The thick lines are output smoothed to remove interannual variability. The black dashed line indicates the 1980 value of the smoothed PF_A1_2010 simulation. The inset shows TCO and 3°S–3°N 20 hPa U-wind. (b) Same as Figure 7a but for 25°S–25°N. The inset shows TCO for 25°S–25°N and 20°S–20°N tropical SSTs with reversed scale.

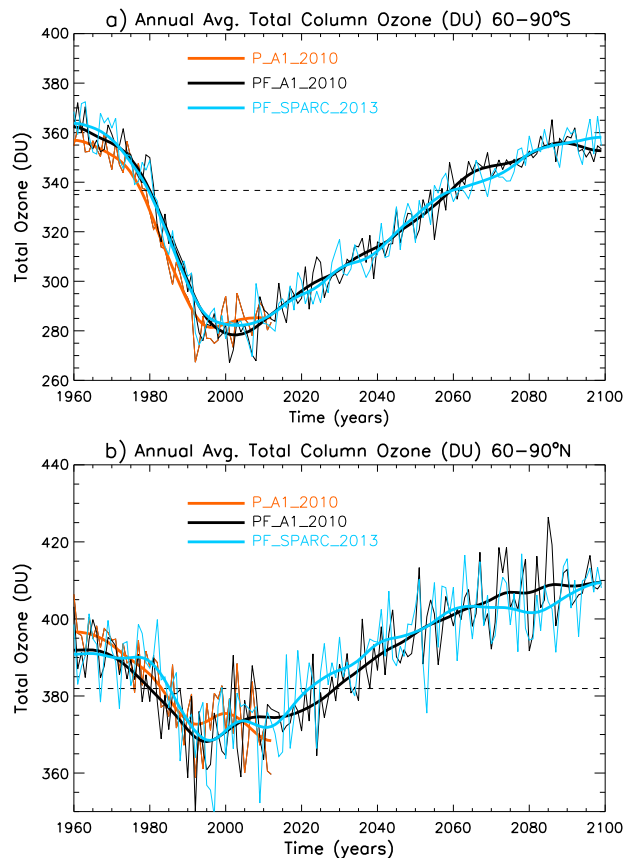


Figure 8. Annual average (a) southern polar cap (60–90°S) and (b) northern polar cap (60–90°N) total column ozone (DU) for P_A1_2010 (orange curve), PF_A1_2010 (black curve), and PF_SPARC_2013 (light blue curve) simulations. P_A1_2010 simulation is from 1960 to 2012; the PF_A1_2010 and PF_SPARC_2013 simulations are from 1960 to 2099. The thick lines are output smoothed to remove interannual variability. The black dashed line indicates the 1980 value of the smoothed PF_A1_2010 simulation.

run. These differences are less than 1 DU on average. All three simulations show that the prominent decrease in ozone follows the Mount Pinatubo eruption [Aquila *et al.*, 2013] in 1991.

Tropical TCO can be significantly impacted by changes in tropical upwelling [Li *et al.*, 2009] as well as by changes in ODSs. Lin and Fu [2013] have shown that the Brewer-Dobson Circulation has multiple branches including the following: a transition zone between the troposphere and stratosphere, a shallow branch between 70 and 30 hPa, and a deep branch above 30 hPa. Processes such as El Niño–Southern Oscillation, or more generally tropical SST anomalies, and the QBO can impact different branches of this circulation. This new version of GEOSCCM includes a realistic QBO, which modulates tropical upwelling and thereby impacts ozone concentrations. Figure 7a shows the annual average TCO over the deep tropics (10°S–10°N) for the three simulations, revealing strong interannual variability. The inset shows an expansion of 2070–2090 with the PF_A1_2010 simulations deep tropical TCO (10°S–10°N) and the 20 hPa U-wind (3°S–3°N), clearly revealing the close relationship of TCO with the QBO in this region. The QBO winds induce a secondary meridional circulation, so that deep tropical upwelling changes are largely balanced by subtropical changes in the opposite direction. This circulation acts to diminish the ozone change due to the QBO when averaged over the broader tropics. Figure 7b shows that the interannual variability in TCO due to the QBO is significantly reduced for a wider tropical average (25°S–25°N). Over this region tropical SSTs dominate the impact on tropical upwelling variability and consequently TCO variability. The inset in Figure 7b shows an expansion of 2070–2090 with the PF_A1_2010 simulations broad tropical TCO (25°S–25°N) and tropical SSTs (20°S–20°N) with a reversed scale as the two are anticorrelated. This can also be seen in the PF_A1_2010 (black thin curve) and

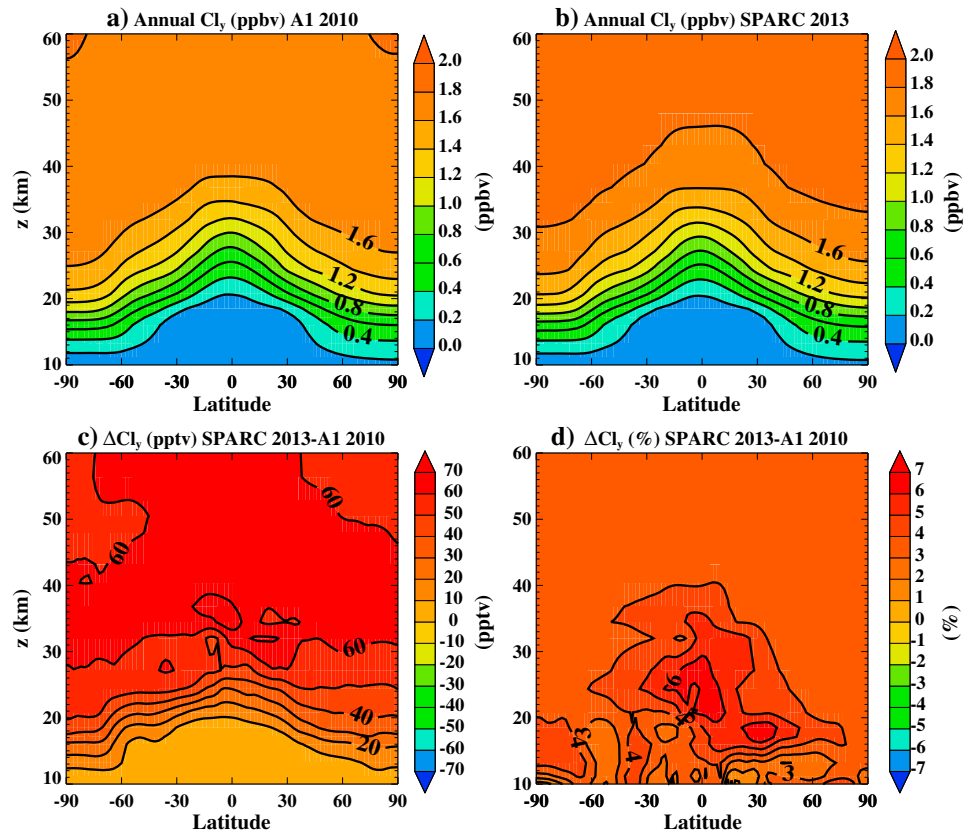


Figure 9. The 2050–2080 annual average Cl_y (ppbv) for (a) the PF_A1_2010 simulation and (b) the PF_SPARC_2013 simulation. The difference in Cl_y between these two simulations is shown in (c) pptv and (d) percent.

PF_SPARC_2013 (light blue thin curve) simulations that show strongly correlated variability forced with identical SSTs. During the second half of the 21st century the PF_SPARC_2013 simulation tends to have slightly less ozone than the PF_A1_2010 simulation which, like the difference in the quasi-global TCO, is less than 1 DU on average. This is again quantitatively consistent with the slightly larger halogen loading in the PF_SPARC_2013 simulation.

Both regions also show slightly larger TCO when observed SSTs are used over modeled ones. This is consistent with the slightly reduced tropical upwelling simulated with slightly cooler observed SSTs compared to modeled SSTs. In both regions of the tropics TCO does not recover to pre-1980s levels by 2100 due to the increasing Brewer-Dobson circulation. In GEOSCCM the increase in circulation dominates over the impact of cooling stratospheric temperatures in tropical total column ozone [Vaughn *et al.*, 2009]. For upper stratospheric ozone, cooling dominates [Li *et al.*, 2009], by slowing the temperature-dependent ozone loss processes [Haigh and Pyle, 1982].

Figure 8a shows the annual SH polar (60–90°S) average TCO evolution for the three simulations. TCO evolution from PF-A1_2010 and PF-SPARC_2013 are similar, with no statistically significant differences between them. In contrast to the tropical and quasi-global TCO, the P_A1_2010 tends to produce less ozone at SH high latitudes at least prior to 1995. Figure 8b shows that over the NH polar region (60–90°N) the high interannual variability and relatively small difference in ODS scenario do not allow the simulations to be distinguishable. An ensemble of simulations would be necessary to see a significant impact from the higher halogen loading in the SPARC 2013 scenario at high latitudes.

3.4. The 2050–2080 Cl_y and Ozone

The differences between the two ODS scenarios are largest during the second half of the 21st century when EESC is expected to recover to 1980 levels. On an annual basis ozone is projected to recover

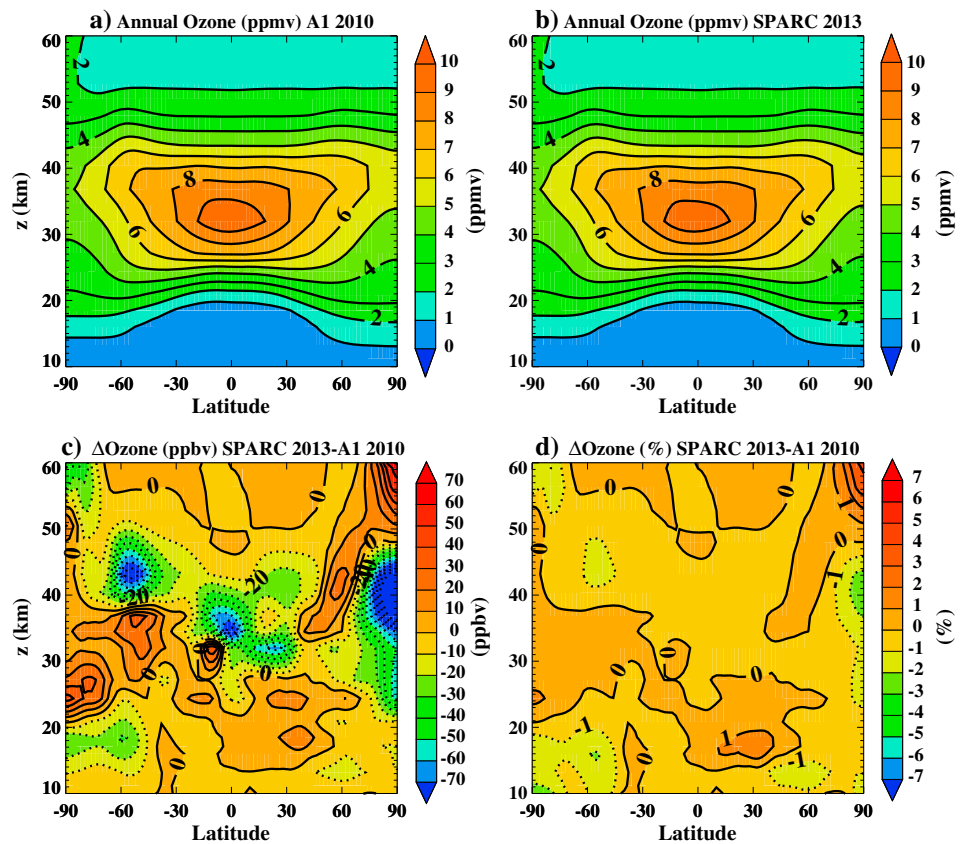


Figure 10. The 2050–2080 ozone (ppmv) annual average for (a) the PF_A1_2010 simulation and (b) the PF_SPARC_2013 simulation. The difference in ozone between these two simulations is shown in (c) ppbv and (d) percent.

somewhat sooner as seen in Figure 8. Figures 9a and 9b show the annual average 2050–2080 Cl_y concentration (ppbv) for the A1 2010 and SPARC 2013 ODS scenarios, respectively. The difference in the two scenarios is shown in Figures 9c and 9d for absolute (pptv) and relative (%) difference, respectively. In the upper stratosphere a 60 pptv increase in Cl_y is simulated in the PF_SPARC_2013 run, which is about a 3–4% difference. This difference is consistent with that seen in *Velders and Daniel* [2014].

The ozone concentrations (ppmv) for the same time period are shown in Figures 10a and 10b for the A1 2010 and SPARC 2013 scenarios, respectively. The difference in ozone is less than 50 ppbv (Figure 10c) over much of the stratosphere, which is generally less than 2% (Figure 10d). A large ensemble would be required to obtain statistically significant differences, especially at high latitudes.

4. Conclusions

Improvements to GEOSCCM since *Pawson et al.* [2008] have on the whole led to significant reductions in ozone biases. GEOSCCM now includes an internally generated QBO, which has improved the tropical interannual variability. The increase in the maximum solar zenith angle from 90 to 94° as the demarcation of day/night chemistry led to a significant reduction in the high-latitude ozone bias. Also, the addition of 5 ppt of Br_y further reduced the bias especially in the SH polar region during August and September.

The GEOSCCM quasi-global (60°S–60°N) total column ozone now compares well to ground-based estimates, especially over the last 30 years. Including observed stratospheric sulfate surface area densities, and combined with the extra Br_y , increases the ozone loss following the Mount Pinatubo eruption and causes the largest average ozone loss in the model to occur during the 1990s as observed, instead of near 2000 in the previous simulations that lack this sulfate variability.

The rate of tropical upwelling increase has decreased moving from the GEOS-4 to GEOS-5 modeling framework with identical SSTs and GHG concentrations. The smaller differences between GEOS-5_old_m and GEOS-5_new_m are largely due to the different SSTs and GHGs that were used in those runs.

We used GEOS-5_new to produce simulations with the A1 2010 and SPARC 2013 ODS scenarios. In the SPARC 2013 scenario there is 60 pptv increase of total chlorine over the previous scenario by 2100, and about 72% of this change comes from F11 changes. This difference is most apparent in the second half of the 21st century and leads to relatively small differences in the quasi-global ozone, typically less than 1 DU.

Within the deep tropics (10°S–10°N) the interannual variability is dominated by the QBO. Over the broader tropics (25°S–25°N) much of the QBO-induced variability in the deep tropics is balanced by opposing changes in the subtropics, leading to relatively smaller net ozone changes. Here tropical SST-induced variability dominates. Ozone in the tropics does not return to pre-1980 levels by 2100 due to circulation changes. Although the SPARC 2013 scenario increases extratropical Cl_y by 3–4% by 2050–2080, its impact on high-latitude ozone is much smaller than the effect of interannual dynamical variability. At high latitudes, an ensemble of simulations is required to quantify the extra Cl_y impact on ozone.

For 21st century ozone projections it is important to understand what model biases impact the response to a perturbation and which do not. *Douglass et al.* [2012] demonstrated that background upper stratospheric temperatures and NO_y values influenced the ozone response to a chlorine perturbation. The changes discussed here do not significantly influence these quantities and mainly impact background ozone concentrations and its variability.

Acknowledgments

The NASA MAP program supported this research. We would like to thank Susan Strahan for helpful comments on this manuscript and Guus Velders for providing the new ODS scenario. We would like to thank four anonymous reviewers for their helpful comments and suggestions for improving this manuscript. We would also like to thank those involved in model development at GSFC and the high-performance computing resources that were provided by NASA's Advanced Supercomputing Division.

References

- Aquila, V., L. D. Oman, R. Stolarski, A. R. Douglass, and P. A. Newman (2013), The response of ozone and nitrogen dioxide to the eruption of Mt. Pinatubo at southern and northern midlatitudes, *J. Atmos. Sci.*, *70*(3), 894–900, doi:10.1175/JAS-D-12-0143.1.
- Baldwin, M. P., et al. (2001), The quasi-biennial oscillation, *Rev. Geophys.*, *39*(2), 179–229, doi:10.1029/1999RG000073.
- Bhartia, P. K., R. D. McPeters, L. E. Flynn, S. Taylor, N. A. Kramarova, S. Frith, B. Fisher, and M. DeLand (2013), Solar backscatter UV (SBUV) total ozone and profile algorithm, *Atmos. Meas. Tech.*, *6*, 2533–2548, doi:10.5194/amt-6-2533-2013.
- Butchart, N., et al. (2011), Multimodel climate and variability of the stratosphere, *J. Geophys. Res.*, *116*, D05102, doi:10.1029/2010JD014995.
- Daniel, J. S., S. Solomon, and D. L. Albritton (1995), On the evaluation of halocarbon radiative forcing and global warming potentials, *J. Geophys. Res.*, *100*(D1), 1271–1285, doi:10.1029/94JD02516.
- Douglass, A. R., R. S. Stolarski, S. E. Strahan, and L. D. Oman (2012), Understanding differences in upper stratospheric ozone response to changes in chlorine and temperature as computed using CCMVal-2 models, *J. Geophys. Res.*, *117*, D16306, doi:10.1029/2012JD017483.
- Engel, A., et al. (2009), Age of stratospheric air unchanged within uncertainties over the past 30 years, *Nat. Geosci.*, *2*, 28–31.
- Eyring, V., et al. (2006), Assessment of temperature, trace species and ozone in chemistry-climate model simulations of the recent past, *J. Geophys. Res.*, *111*, D22308, doi:10.1029/2006JD007327.
- Eyring, V., et al. (2013), Overview of IGAC/SPARC Chemistry-Climate Model initiative (CCMI) community simulations in support of upcoming ozone and climate assessments, SPARC Newsletter No. 40, p. 48–66.
- Fioletov, V. E., G. E. Bodeker, A. J. Miller, R. D. McPeters, and R. Stolarski (2002), Global ozone and zonal total ozone variations estimated from ground-based and satellite measurements: 1964–2000, *J. Geophys. Res.*, *107*(D22), 4647, doi:10.1029/2001JD001350.
- Fioletov, V. E., et al. (2008), The performance of the ground-based total ozone network assessed using satellite data, *J. Geophys. Res.*, *113*, D14313, doi:10.1029/2008JD009809.
- Garfinkel, C. I., A. M. Molod, L. D. Oman, and I.-S. Song (2011), Improvement of the GEOS-5 AGCM upon updating the air-sea roughness parameterization, *Geophys. Res. Lett.*, *38*, L18702, doi:10.1029/2011GL048802.
- Garfinkel, C. I., L. D. Oman, E. A. Barnes, D. W. Waugh, M. M. Hurwitz, and A. M. Molod (2013), Connections between the spring breakup of the Southern Hemisphere polar vortex, stationary waves, and air-sea roughness, *J. Atmos. Sci.*, *70*(7), 2137–2151, doi:10.1175/JAS-D-12-0242.1.
- Gent, P. R., et al. (2011), The Community Climate System Model version 4, *J. Clim.*, *24*(19), 4973–4991, doi:10.1175/2011JCLI4083.
- Gillett, N., and D. W. J. Thompson (2003), Simulation of recent Southern Hemisphere climate change, *Science*, *302*, 273–275.
- Haigh, J. D., and J. A. Pyle (1982), Ozone perturbation experiments in a two-dimensional circulation model, *Q. J. R. Meteorolog. Soc.*, *108*, 5510–574, doi:10.1002/qj.49710845705.
- Hurwitz, M. M., L. D. Oman, P. A. Newman, and I.-S. Song (2013), Net influence of an internally generated quasi-biennial oscillation on modeled stratospheric climate and chemistry, *Atmos. Chem. Phys.*, *13*, 12187–12197.
- Kawatani, Y., and K. Hamilton (2013), Weakened stratospheric quasi-biennial oscillation driven by increased tropical mean upwelling, *Nature*, *497*(7450), 478–481, doi:10.1038/nature12140.
- Kaye, J. A., S. A. Penkett, and F. M. Ormond (Eds) (1994), *Report on Concentrations, Lifetimes, and Trends of CFCs, Halons, and Related Species*, vol. 1339, NASA, Washington, D. C.
- Lamago, D., M. Dameris, C. Schnadt, V. Eyring, and C. Bruhl (2003), Impact of large solar zenith angles on lower stratospheric dynamical and chemical processes in a coupled chemistry-climate model, *Atmos. Chem. Phys.*, *3*, 1981–1990.
- Li, F., R. S. Stolarski, and P. A. Newman (2009), Stratospheric ozone in the post-CFC era, *Atmos. Chem. Phys.*, *9*, 2207–2213, doi:10.5194/acp-9-2207-2009.
- Liang, Q., R. S. Stolarski, S. R. Kawa, J. E. Nielsen, J. M. Rodriguez, D. R. Blake, E. L. Atlas, and L. E. Ott (2010), Finding the missing stratospheric Br_y: A global modeling study of CHBr₃ and CH₂Br₂, *Atmos. Chem. Phys.*, *10*, 2269–2286.
- Lin, P., and Q. Fu (2013), Changes in various branches of the Brewer-Dobson circulation from an ensemble of chemistry climate models, *J. Geophys. Res. Atmos.*, *118*, 73–84, doi:10.1029/2012JD018813.

- McFarlane, N. (2008), Connections between stratospheric ozone and climate: Radiative forcing, climate variability, and change, *Atmos. Ocean*, 46(1), 139–158, doi:10.3137/ao.460107.
- Meinshausen, M., et al. (2011), The RCP greenhouse gas concentrations and their extensions from 1765 to 2300, *Clim. Change*, 109(1–2), 213–241.
- Molod, A., L. Takacs, M. Suarez, J. Bacmeister, I.–S. Song, and A. Eichmann (2012), The GEOS–5 atmospheric general circulation model: Mean climate and development from MERRA to Fortuna, Technical Report Series on Global Modeling and Data Assimilation, vol. 28. [Available at: <http://gmao.gsfc.nasa.gov/pubs/docs/Molod484.pdf>.]
- Moss, R. H., et al. (2010), The next generation of scenarios for climate change research and assessment, *Nature*, 463(7282), 747–756.
- Newman, P. A., J. S. Daniel, D. W. Waugh, and E. R. Nash (2007), A new formulation of equivalent effective stratospheric chlorine (EESC), *Atmos. Chem. Phys.*, 7, 4537–4552, doi:10.5194/acp-7-4537-2007.
- Oman, L. D., et al. (2010), Multi-model assessment of the factors driving stratospheric ozone evolution over the 21st century, *J. Geophys. Res.*, 115, D24306, doi:10.1029/2010JD014362.
- Pawson, S., R. S. Stolarski, A. R. Douglass, P. A. Newman, J. E. Nielsen, S. M. Frith, and M. L. Gupta (2008), Goddard Earth Observing System chemistry-climate model simulations of stratospheric ozone-temperature coupling between 1950 and 2005, *J. Geophys. Res.*, 113, D12103, doi:10.1029/2007JD009511.
- Randel, W. J., and A. M. Thompson (2011), Interannual variability and trends in tropical ozone derived from SAGE II satellite data and SHADOZ ozonesondes, *J. Geophys. Res.*, 116, D07303, doi:10.1029/2010JD015195.
- Ray, E. A., et al. (2010), Evidence for changes in stratospheric transport and mixing over the past three decades based on multiple datasets and tropical leaky pipe analysis, *J. Geophys. Res.*, 115, D21304, doi:10.1029/2010JD014206.
- Rienecker, M. M., et al. (2008), The GEOS-5 data assimilation system—Documentation of versions 5.0.1, 5.1.0, and 5.2.0. Technical Report Series on Global Modeling and Data Assimilation, 27.
- Stratosphere-troposphere Processes and their Role in Climate (SPARC) (2013), Report on the lifetimes of stratospheric ozone-depleting substances, their replacements, and related species, *SPARC Rep. 6, WCRP-15/2013*, edited by M. Ko et al.
- SPARC Chemistry-Climate Model Validation (CCMVal) (2010), SPARC CCMVal report on the evaluation of chemistry-climate models, *SPARC Rep. 5, WCRP-132, WMO/TD-No. 1526*, edited by V. Eyring et al. [Available at <http://www.atmosph.physics.utoronto.ca/SPARC/>.]
- Stolarski, R. S., and S. M. Frith (2006), Search for evidence of trend slow-down in the long-term TOMS/SBUV total ozone data record; the importance of instrument drift uncertainty, *Atmos. Chem. Phys.*, 6, 4057–4065.
- Strahan, S. E., et al. (2011), Using transport diagnostics to understand chemistry climate model ozone simulations, *J. Geophys. Res.*, 116, D17302, doi:10.1029/2010JD015360.
- Velders, G. J. M., and J. S. Daniel (2014), Uncertainty analysis of projections of ozone-depleting substances: Mixing ratios, EESC, ODPs, and GWPs, *Atmos. Chem. Phys.*, 14, 2757–2776, doi:10.5194/acp-14-2757-2014.
- Waugh, D. W., L. Oman, S. R. Kawa, R. S. Stolarski, S. Pawson, A. R. Douglass, P. A. Newman, and J. E. Nielsen (2009), Impact of climate change on stratospheric ozone recovery, *Geophys. Res. Lett.*, 36, L03805, doi:10.1029/2008GL036223.
- World Meteorological Organization (2011), Scientific assessment of ozone depletion: 2010, Global Ozone Research and Monitoring Project-Report No. 52, 516 pp., Geneva, Switzerland.
- Ziemke, J. R., S. Chandra, and P. K. Bhartia (2005), A 25-year data record of atmospheric ozone in the Pacific from Total Ozone Mapping Spectrometer (TOMS) cloud slicing: Implications for ozone trends in the stratosphere and troposphere, *J. Geophys. Res.*, 110, D15105, doi:10.1029/2004JD005687.